VTT Technical Research Centre of Finland

Characterizing the UAV-to-Machine UWB Radio Channel in Smart Factories

Semkin, Vasilii; Vitucci, Enrico Maria; Fuschini, Franco; Barbiroli, Marina; Degli-Esposti, Vittorio; Oestges, Claude

Published in:
IEEE Access

DOI:
10.1109/ACCESS.2021.3082312

Published: 01/01/2021

Document Version
Publisher's final version

IEEE Access
Multidisciplinary | Rapid Review | Open Access Journal

Received April 19, 2021, accepted May 17, 2021, date of publication May 20, 2021, date of current version June 1, 2021.

Digital Object Identifier 10.1109/ACCESS.2021.3082312

Characterizing the UAV-to-Machine UWB Radio Channel in Smart Factories

VASILII SEMKIN[1,2], ENRICO MARIA VITUCCI[3], (Senior Member, IEEE), FRANCO FUSCHINI[3], MARINA BARBIROLI[3], VITTORIO DEGLI-ESPOSTI[3], (Senior Member, IEEE), AND CLAUDE OESTGES[1], (Fellow, IEEE)

[1]Institute for Information and Communication Technologies, Electronics and Applied Mathematics (ICTEAM), Université catholique de Louvain, 1348 Louvain-la-Neuve, Belgium
[2]VTT Technical Research Centre of Finland Ltd., 02150 Espoo, Finland
[3]Department of Electrical, Electronic and Information Engineering "Guglielmo Marconi" (DEI), CNIT, University of Bologna, 40136 Bologna, Italy

Corresponding author: Vasilii Semkin (vasilii.semkin@vtt.fi)

This work was supported in part by the FRS-FNRS (Fonds de la Recherche Scientifique), Belgium, through the Research Project MACHAON, in part by EOS (Excellence of Science) project MUSEWINET (MUlti SErvice WIreless NETworks), in part by the Academy of Finland, in part by the Italian Ministry of University and Research (MUR) through the programme "Dipartimenti di Eccellenza (2018–2022)—Precision Cyberphysical Systems Project (P-CPS)," and in part by the Eu COST Action IRACON (Inclusive Radio Communication Networks for 5G and Beyond) under Grant CA15104. The work of Vasilii Semkin was supported in part by the Jorma Ollila grant.

ABSTRACT In this work, the results of Ultra-Wideband air-to-ground measurements carried out in a real-world factory environment are presented and discussed. With intelligent industrial deployments in mind, we envision a scenario where the Unmanned Aerial Vehicle can be used as a supplementary tool for factory operation, optimization and control. Measurements address narrow band and wide band characterization of the wireless radio channel, and can be used for link budget calculation, interference studies and time dispersion assessment in real factories, without the usual limitation for both radio terminals to be close to ground. The measurements are performed at different locations and different heights over the 3.1–5.3 GHz band. Some fundamental propagation parameters values are determined vs. distance, height and propagation conditions. The measurements are complemented with, and compared to, conventional ground-to-ground measurements with the same setup. The conducted measurement campaign gives an insight for realizing wireless applications in smart connected factories, including UAV-assisted applications.

INDEX TERMS UAV, RF channel measurements, UWB radio propagation, smart factory, conscious factory, automation.

I. INTRODUCTION

Nowadays, Unmanned Aerial Vehicles (UAVs), also known as drones, are utilized across a wide range of applications. UAVs introduce new opportunities and increase efficiency in mapping, forensics, visual support for first responders, etc. [1]–[4]. An interesting possible application includes UAV utilization in industrial environments. UAVs can facilitate the appearance of new industrial management practices, allowing gathering visual data and performing optimization and control tasks very efficiently, without the need for humans to patrol large, often noisy and sometimes unsafe, industrial premises.

Lately, smart (or "conscious") factories with pervasively connected machines are attracting attention from many industries. The work of different interconnected machines and robots can be optimised and provides economical benefits for companies [5]. UAVs, integrated with the other machines can have extensive capabilities in manufacturing processes, units delivery, supervision, or can even be used to manage and optimize other connected machines, as shown in Fig. 1. The supervising UAV will be operated from the control point. The operator will collect information from the sensors and connected machines about the status of current and future tasks, analyzing factory efficiency and possible problems. If the operator of the factory receives data about defective or inefficient machine operation, the supervising UAV can be sent on place to provide visual data and direct connection between the malfunctioning robot and the operator. This application requires stable wireless connection to the UAV, and the chance that the link is blocked by machines or disturbed by poor propagation conditions must be minimized. Although the idea of conscious factory was already presented by Nokia and discussed in [6] in terms of human-robot interaction,

The associate editor coordinating the review of this manuscript and approving it for publication was Abderrahmane Lakas.

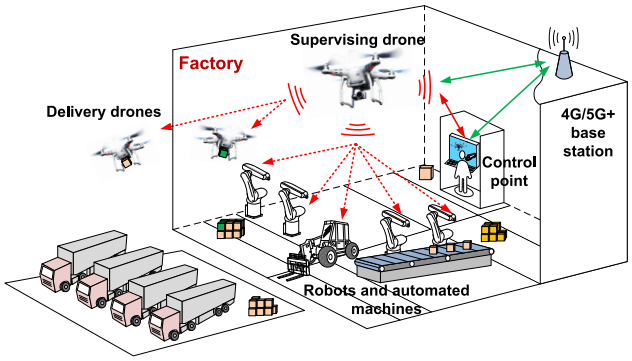

FIGURE 1. Our vision on the UAV integration into the future fully automated conscious factory.

(a) Photograph of the factory

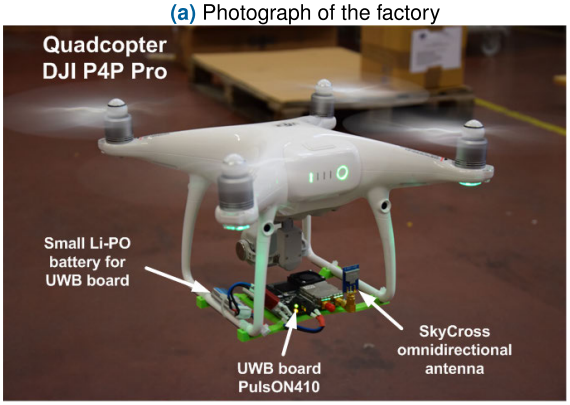

(b) Photograph of the flying UAV

FIGURE 2. Phantom UAV with the transmitting UWB board and the environment of interest.

to the best authors' knowledge there are no focused studies on radio wave propagation in a factory environment between UAVs and other machines. This is the main reason why we decided to carry out the present work on UAV-to-machine UWB propagation characterization in industrial environment.

Ultra-Wide Band (UWB) technology is an established short range communication technology based on the IEEE 802.15.4a/z standard [7]: numerous applications, including industrial environments, can utilize and benefit from it [8]. UWB radio systems operate in the unlicensed frequency band from 3.1 to 10.6 GHz and offer expedient opportunities for short-range dependable communications at a very low cost. UWB communication systems are of interest also for the large bandwidth available and the low interference due to their low spectral density [9], [10]. In addition, UWB communications can be used to serve a large number of users and to achieve a high multi-path resolution, and can be, therefore, a good candidate for the rich scattering industrial environment, where high-reliability wireless communication is required. Moreover, UWB transmission can empower accurate radio location that can be very important in smart factory applications [11]. The exploitation of the UWB high-accuracy localization potential however, as well as the study of propagation in other frequencies bands, e.g. millimeter-wave bands that will be used in next generation wireless systems, are not covered in the present paper but is a part of our future research.

The communication channel in the UWB frequency band has been thoroughly studied in the past [12]–[17]. In [12] and [18] the authors present Ultra-Wide Band (UWB) channel measurements in an industrial environment along with the analysis of small-scale fading statistics, while in [15] and [16], the path loss exponent for UWB propagation is evaluated in residential and in-home environments, respectively. In another work presented in [19], the authors study the industrial indoor channel using fixed positions of the Tx and the Rx at different frequencies, including 5.2 GHz which is a part of the UWB. The obtained path loss exponent values that depend on the environment, e.g. LOS or obstructed LOS (light clutter or heavy clutter) are similar to that one's measured in this work and are discussed in Section III.

Although UWB propagation in general has been widely studied, UWB between UAVs and any other machines in industrial environment is barely studied. A few research works study air-to-ground channel properties in indoor environments. In [20] the authors study communication between UAV and wearable device at UWB frequencies, but the studied environment is an empty warehouse with the metallic walls, therefore very low path loss exponent values are obtained. Most investigations involving UAVs for indoor use are focused on positioning and navigation studies [21], [22]. On the other hand there are many studies related to air-to-ground propagation in outdoor environments, as shown in the following survey [23].

In the present work, we specifically focus on air-to-ground (i.e., UAV-to-robot, UAV-to-operator) UWB radio channel characterization in industrial facilities. Besides their many practical applications, UAVs are also formidable tools for performing measurements at hardly reachable elevated points to give better insight on propagation characteristics in this peculiar environment. Our measurements can be of interests even for cases where the use of a UAV is not necessary, but the knowledge of propagation characteristics for radio terminal located at different heights within an indoor, industrial environment is important for designing reliable communications. In addition, we compare these multiple UAV-to-ground measurements with conventional ground-to-ground measurements in the same environment, to highlight the effect of the UAV platform on the channel characteristics.

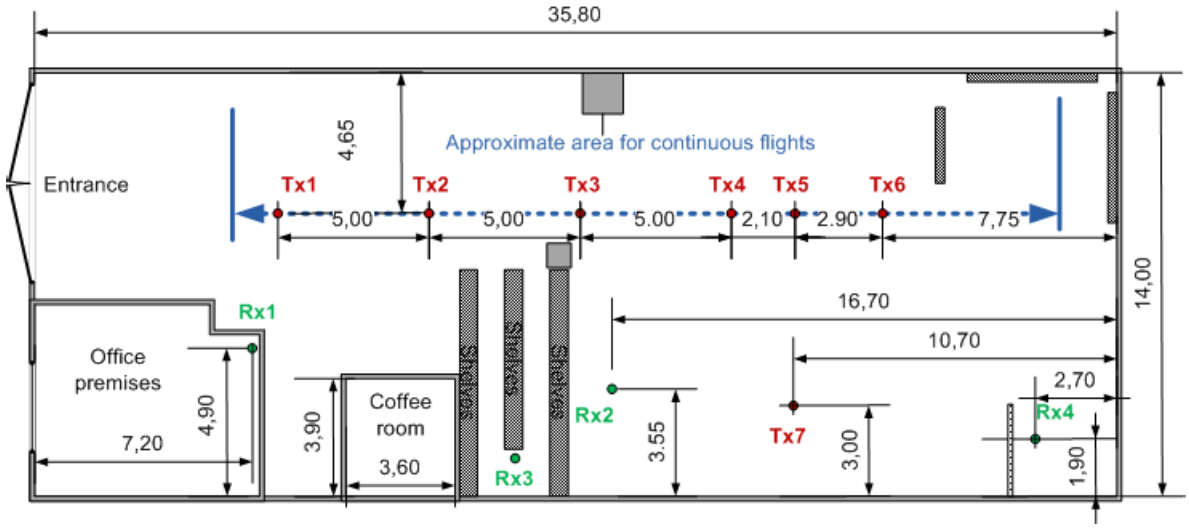

FIGURE 3. Factory floor plan with the dimensions in meters and marked Tx/Rx positions. Green text corresponds to Rx locations, red text to Tx (installed on the UAV) positions.The blue dashed-line corresponds to the route of the drone during continuous-flight measurements.

The structure of this document is as follows: Section II presents the measurement setup overview and a description of the measurement scenario. Section III provides the analysis of the results. Finally, Section IV concludes the paper and discusses plans for the future work.

II. MEASUREMENT EQUIPMENT AND SCENARIO

The measurements were conducted in a functioning Italian factory (Fig. 2, a) focused on design and construction of customized automation systems. The factory realizes the machinery design and assembly, as well as technical assistance, and administers components storage.[1] The overall factory's dimensions are 35.8 m by 14 m (the floorplan is presented in Fig. 3). The ceiling height is approximately 7.5 m.

In this measurement campaign, we utilize the popular consumer UAV DJI Phantom 4 Pro (Fig. 2, b). This UAV is able to carry small weight equipment and has multilateral vision system allowing safe indoor manual control. The side obstacle avoiding system was enabled during the UAV operation. It should be noted that UAV was manually controlled during the measurement campaign, since downwards sensor was blocked by the payload (UWB board) and GPS signal was not available indoors.

The measurements were performed using two UWB boards PulsON410[2] operating from 3.1 to 5.3 GHz. The transmitter (Tx) node was installed under the UAV using a 3D printed fixture. The Tx board was powered with a small Li-Po battery, which is enough for 30 min operating time. The receiver (Rx) node was fixed on the mast at a height of 2 m. The particular receiver position Rx1 however is located in the office on the mezzanine floor at 5.4 m height from the ground floor

[1]http://www.gfautomazioni.it
[2]https://www.humatics.com/

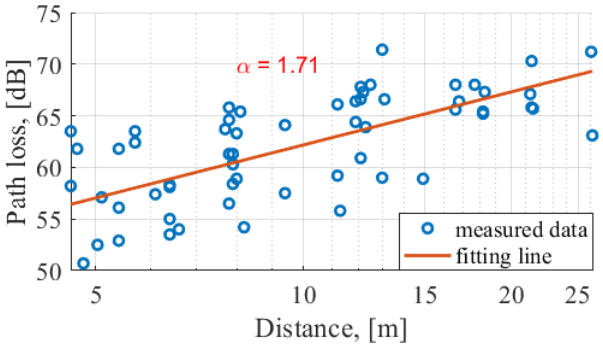

FIGURE 4. Path loss values obtained during all measurements and the corresponding fitting line.

(Fig. 3), to mimic UAV communication with the control room. Omnidirectional antennas were used at both Tx and Rx sides, with an approximate gain of 3 dBi. Static measurements were performed in most cases (i.e. UAV was hovering at the specified locations marked as Tx[.] in Fig. 3). The channel impulse response (CIR) was recorded for approximately 2 minutes at each location to get the statistics and minimize possible interference from people walking around. During one of the surveying sets the UAV was continuously flying back and forth along the specified route and the CIR was recorded during the whole flight (hereafter called dynamic measurements).

A summary table of the UAV-to-ground measurement results is presented in Table 1 and the locations are specified on the floor plan in Fig. 3. The measurements are organized in Table 1 in 3 different data sets, as they have been performed during three campaigns on different dates. Since the factory was operational, there were some differences in the industrial equipment locations. For example, two big metallic

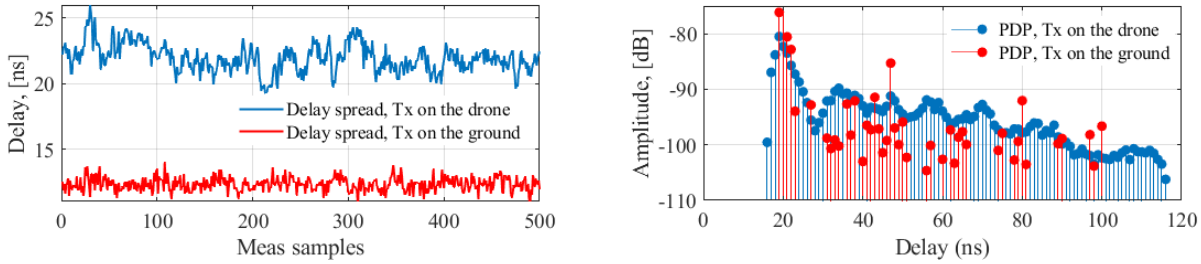

(a) RMS Delay Spread (b) Averaged Power Delay Profile

FIGURE 5. Comparison between UAV and ground measurements for the Tx1-Rx1 setup (blue line - Tx on UAV and red line - Tx on the mast). Rx1 is located upstairs in the office.

cupboards were present only during second measurement set between Tx7 and Rx4 (see Fig. 3). Ground-to-ground measurements (i.e. with the Tx fixed at ground) at several positions were also performed, in order to complement the UAV-to-ground measurements. Also the ground-to-ground measurements were collected in 2 different dates, and they are presented in Table 2, divided into 2 data sets.

III. MEASUREMENT RESULTS

The results are presented and analyzed considering two cases, i.e. static measurements when the UAV is hovering at one of the specified positions and dynamic measurements, when UAV is flying along the factory. In addition, ground-to-ground measurements at several positions are presented: during these measurements the Tx was fixed on the mast at heights of 1, 2, and 3.5 m, respectively. In most cases, the Tx height in ground-to-ground measurements differs from the UAV height in UAV-to-ground measurements in the same locations, except for a few measurements where both the locations and the heights are the same, for the sake of comparison. These additional ground-to-ground measurements (see Table 2) are also analyzed and compared with the static UAV-to-ground measurements in the following sub-section.

A. MEASUREMENTS AT FIXED POSITIONS

The measured path loss, RMS delay spread, average and maximum excess delay values for all Tx and Rx locations, classified into line-of-sight (LOS), quasi-line-of-sight (quasi-LOS) and non-line-of-sight (NLOS) configurations, are presented in Table 1 and Table 2.

The mean RMS delay spread values vary between 9.8 and 49.2 ns, where values lower than 25 ns are mainly observed in LOS or quasi-LOS locations, and values higher than 25 ns in NLOS locations, in a reasonable agreement with [12]. With respect to [12] however, lower delay spread values are obtained sometimes for the LOS and quasi-LOS locations: this might be due to different characteristics of the environment. Although the space considered in this work is larger, there is more cluttering due to machines and metallic shelves generating scattering and obstruction. For some locations (e.g. Tx1-Rx1), the UAV-to-ground measurements have been performed twice in different days and the measured delay

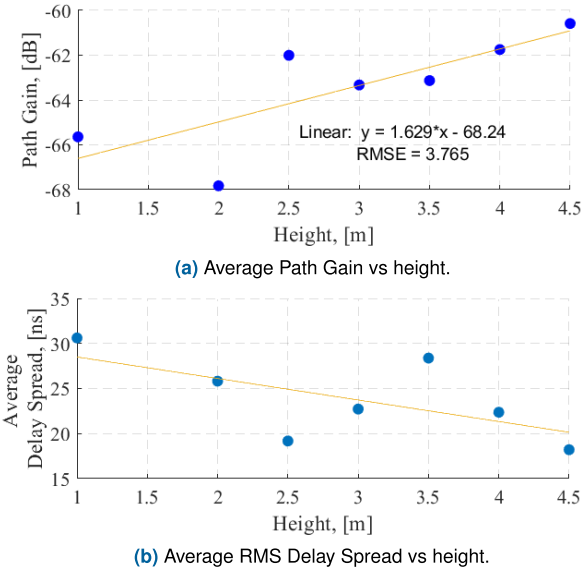

(a) Average Path Gain vs height.

(b) Average RMS Delay Spread vs height.

FIGURE 6. Measured dependence of the average Path Gain and RMS Delay Spread versus height of the transmitter.

spread values differs slightly, probably due to the different position of some machines.

For what concerns path loss, we refer to the well known path-loss exponent model. Specifically, path loss $L(d)$ vs. link-distance is expressed through the following fixed-intercept formula [24]:

$$L(d) = L(d_0) + 10\alpha \log_{10}(d) + X_\sigma, \tag{1}$$

where d is the 3D distance between Tx and Rx, d_0 is a reference distance, α is path loss exponent, and X_σ is a random variable that accounts for shadowing variation modeled using a zero-mean log-normal distribution with standard deviation σ, assumed equal to the standard deviation of the regression residuals [24]. The data are fitted as usual with a line in a log-log plot, as shown in Fig. 4. Altogether, sixty measurements are selected to determine the path loss values: it is worth noticing that the fast fading effect is removed from the data due to the large bandwidth of the UWB equipment and the 2-minutes time-averaging at each static location. Path loss values in different locations have large deviations due to

the rich scattering environment. Although the factory can be considered mostly an open space, the many metal scatterers generate a quasi-reverberant environment. The estimated path loss exponent is equal to 1.71, i.e. lower than free-space, which is rather common for such a type of environment. This value is similar to that ones found in the literature, e.g. [15], [16]. The corresponding value for the standard deviation of the shadowing is $\sigma = 3.8$ dB.

One may observe that the setup when the UAV is hovering replicates static ground measurements when both Tx and Rx are fixed on tripods or masts. The setups are similar, but the UAV suffers from vibrations and some drifting relative to its initial position due to the GPS being blocked by the roof, and the UAV body itself impacts on the multipath structure. As an example, in Fig. 5 we compare RMS delay spread and averaged PDP for the ''UAV-to-ground'' and ''ground-to-ground'' measurements for Tx1-Rx1, with Tx at 2 meters height in both cases. It is clear that results are different for the two cases. Besides drifting, which is evident from the greater irregularity of the curve in Fig. 5(a), the UAV body is affecting the radiation pattern of the antenna and generating reflections or obstructions from the UAV hull. Therefore, the PDP has a denser structure when compared to the corresponding ground-to-ground case: this also corresponds to a higher average Delay Spread value (22 ns vs. 9.8 ns). A similar behaviour can be observed comparing UAV-to-ground vs. ground-to-ground measurements with same height in other locations (e.g. Rx1-Tx2).

However, if we consider the whole measurement dataset in Table 1 (UAV-to-ground measurements) and Table 2 (ground-to-ground measurements), on the average the reported values do not differ much. Considering the average delay spread for all the considered locations, both with Tx on the UAV (Table 1) and Tx on the mast (Table 2), we get an average delay spread value of 18 ns in the LOS and quasi-LOS configurations, and of 28 ns in the NLOS configurations. Regarding path loss, we get an average value of 59 dB in the LOS/quasi-LOS configurations, and of 66 dB in the NLOS configurations. Nevertheless, the measured values in the different Rx locations are strongly influenced by the degree of obstruction caused by shelves and machines, and especially by the Tx height.

In Fig. 6, the dependence of the average normalized power (path gain) and RMS delay spread versus Tx height is presented. Only a subset of the measured data (both UAV-to-ground and ground-to-ground) is considered in this plot: the considered data are marked with a ''*'' in Table 1 and Table 2, and they correspond to those locations that are more representative of typical configurations (LOS, quasi-LOS, and NLOS). Moreover, all the Path Gain values have been realigned to remove the dependence on distance, in order to observe only the effect of Tx height and obstructions. Looking at Fig. 6(a), it is evident that the path gain is linearly increasing for heights above 2.5 m, while for lower heights the deviations from the fitting line are more severe. Being the height of most shelves of the factory approximately 2.5 m, we believe that these fluctuations for lower heights are probably caused by obstructions caused by objects on the shelves. The average RMS Delay Spread (Fig. 6(b)) also varies significantly with the height according to an overall decreasing trend.

B. MEASUREMENTS DURING CONTINUOUS FLIGHT

In this subsection we present the results obtained during the continuous UAV flight at height of approximately 2.5 m. The starting point is located near the entrance and the UAV flies straight to the opposite wall and back, forward and backward for five times. The continuous flight route is represented with a blue dashed line in Fig. 3. The receiver is fixed at position Rx2 (see Fig. 3), at 2 m height. There might be an error of 0.5-1 m in the UAV heights and also along x- and y- coordinates since the UAV was operated manually and was drifting during flight.

In Fig. 7, (blue line) the average measured path gain during continuous UAV flights is shown. The path gain is obtained by integrating the CIR for each snapshot, and averaging the obtained values through a sliding observation windows of about 1 m: after that, the obtained path gain values for the 5 round-trip flights are averaged together. The spatial averaging procedure is necessary to cut-off fast-fading effects and to clearly identify starting points for each flight, so that the subsequent time averaging of the data among the flights becomes more accurate. The speed of the UAV was almost constant for all conducted flights and is equal to approximately 1 m/s. There might be some difference in the beginning and end of the route due to acceleration and braking of the UAV. The averaging procedure previously described can help to compensate for possible different speed at these parts of the route. Besides averaging, the standard deviation of the collected data for each reference point of the route is also computed, and represented through vertical error bars in Fig. 7 (the length of the vertical bars is equal to double the standard deviation).

Looking at Fig. 3, we observe that the initial UAV position has no LOS link and moreover, there are many shelves between Tx and Rx. In fact, as the UAV flies towards the end wall, the power level (path gain) shown in Fig. 7 increases and reaches a maximum for the (quasi)-LOS case when UAV is in the middle of the route at approximately 10m from the starting point, i.e. when the Tx-Rx distance is minimum. Then the power level drops due to the increasing distance between Tx and Rx and some machines obstructing the link, but not as much as for the first part of the route.

In Fig. 7 (red line), the mean and standard deviation values of the delay spread are also presented, for the forward and backward UAV flights. The measured average delay spread for continuous UAV flight varies from 10 ns to 23 ns.

Interestingly, the standard deviation of both path loss and delay spread is greater in the central part of the graph: this is probably due to the quasi-LOS nature of the locations in this section, where obstructing objects can generate intermittent shadowing and therefore a great variability.

TABLE 1. Summary of the performed measurements with Tx on UAV.

Meas. Set	UAV (Tx) Pos.	Rx Pos.	Scenario Type	UAV (Tx) Height, [m]	Tx-Rx Dist., [m]	Mean Path Loss, [dB]	Mean Excess Delay, [ns]	Max Excess Delay, [ns]	RMS Delay Spread, [ns]
№1	Tx7	Rx3	NLOS	4	5.4	61.8	31.7	95.7	18.6
	Tx2		NLOS	2	7.9	60.3	27.8	90.2	13.7
	Tx1		NLOS	2	12.1	60.9	29	94.4	15.1
	Tx1		NLOS	4	12.3	63.9	31.7	95.7	17.1
	Tx6	Rx1	NLOS	2	21.3	67.1	31.4	107.1	21.9
	Tx7 *		NLOS	4	16.6	65.6	36.1	97.8	24.4
	Tx3 *		NLOS	4	11.9	64.4	41.3	98.6	23.2
	Tx2 *		Q-LOS	4	7.7	63.7	42	95.1	24.2
	Tx1 *		Q-LOS	2	5.7	62.4	27.2	94.2	16.7
	Tx1 *		Q-LOS	4	4.7	61.8	32.9	95.7	20.2
№2	Tx1 *	Rx2	NLOS	2.5	12.1	67.8	34.7	100.8	20.8
	Tx2 *		NLOS	2.5	7.9	61.3	28.6	94.2	15.5
	Tx3		Q-LOS	2.5	5.1	57.1	26.5	74.5	12.4
	Tx4 *		LOS	2.5	6.4	58.3	27.6	91.8	15.4
	Tx7		LOS	2.5	6.1	57.4	30	93.2	20.8
	Tx5		LOS	4.5	8.2	54.2	23.5	83.1	11.2
	Cont. flight		—	2.5	5 - 15	53 - 66	19.5 - 47.2	54 - 114	10 - 23
№3	Tx1	Rx4	NLOS	2	26.1	71.2	33.6	114.1	24.9
	Tx2 *		NLOS	2.5	21.4	65.8	41.2	108.8	25
	Tx3		NLOS	2.25	16.8	66.4	47.7	109.8	17.7
	Tx4		Q-LOS	2.5	12.5	68	42	112.4	14.7
	Tx7		Q-LOS	3	8.1	65.4	34.6	96.3	18.3
	Tx1		NLOS	4.25	26.2	63.1	32.3	103.4	19
	Tx5		Q-LOS	4.75	11.3	55.8	27.2	86.6	13.4
	Tx1 *	Rx1	Q-LOS	2	5.7	63.5	34.9	102.2	22
	Tx1 *		Q-LOS	4.5	4.6	58.2	31.2	87.2	17.4
	Tx2 *		Q-LOS	2.75	7.8	65.8	41.2	108.8	22.1
	Tx3		NLOS	2.5	11.9	66.4	47.7	109.8	24.1
	Tx4		NLOS	2.5	16.6	68	42	112.4	26.8
	Tx5 *		NLOS	4.5	17.7	68	43.7	112.8	26.2
	Tx7 *		NLOS	2.75	18.2	65.4	34.6	96.3	23.4

C. COMPARISON WITH PREVIOUS WORKS

The work [25], summarizes the results from many UWB indoor measurement campaigns (in office, classroom, laboratory environment, etc.) and shows that the path loss exponent values are in between 1.3 and 2.4 for LOS case, while typical values above 1.7 are found in the NLOS cases. Another work [26], analyses narrowband measurement results obtained in five factories at ultra-high frequencies, i.e. 1.3 GHz: the obtained path loss exponent values are equal to 1.79 for LOS cases (light and heavy clutter). In general, values lower than 2 are quite common in some indoor scenarios (e.g. corridors or large rooms), because the confined environment allows the establishment of waveguiding effects.

According to [24], the following path loss exponent values are expected in different environments at frequencies below 6 GHz:

- Urban area cellular radio (non-shadowed)=2.7-3.5
- Shadowed urban cellular radio=3-5
- In-building LOS=1.6-1.8
- Obstructed LOS in-building=4-6
- Obstructed LOS in factories=2-3

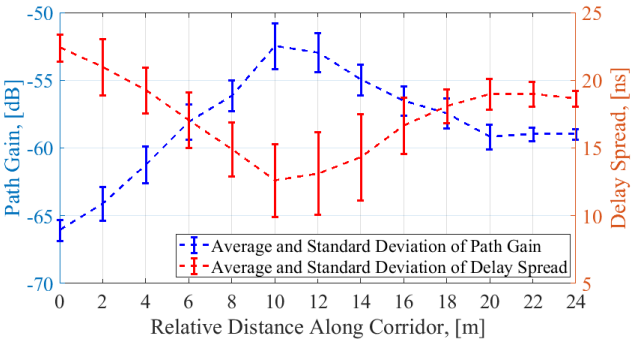

FIGURE 7. Average and standard deviation of the path gain and delay spread during continuous UAV flights.

Based on the information presented above, initially, we expected to get a path loss exponent value from 1.6 up to a maximum of 3. However, due to large open spaces in the factory and high probability of LOS communication, since in most cases the UAV is flying higher than average shelf height, the obtained path loss exponent value is

TABLE 2. Summary of the performed measurements with Tx at ground.

Meas. Set	Tx Pos.	Rx Pos.	Scenario Type	Tx Height, [m]	Tx-Rx Dist., [m]	Mean Path Loss, [dB]	Mean Excess Delay, [ns]	Max Excess Delay, [ns]	RMS Delay Spread, [ns]
№1	Tx1 *	Rx1	Q-LOS	3.5	4.7	50.7	21.8	52.9	9.8
	Tx1 *		Q-LOS	2	5.7	58.8	23.3	81.9	12.3
	Tx2 *		Q-LOS	3.5	7.7	58.9	42.4	177.4	24.5
	Tx2 *		Q-LOS	2	8	60.1	22.1	68.8	10.1
	Tx7 *		NLOS	3.5	16.6	67.3	35.1	151.6	27.9
	Tx7 *		NLOS	2	16.5	67.8	36.1	184.1	31.2
	Tx1 *	Rx2	NLOS	3.5	12.1	67.3	49.7	215.6	49.2
	Tx2 *		NLOS	3.5	8	63.3	45.1	201	37.7
	Tx4 *		LOS	3.5	6.5	54	24.5	91.2	13.4
	Tx1	Rx4	NLOS	3.5	26.1	66.6	37.1	211.8	32.7
	Tx2 *		NLOS	3.5	21.4	65.7	41.5	207.2	33.6
	Tx2 *		NLOS	2	21.4	74.4	49.9	216.7	40.9
№2	Tx1 *	Rx1	Q-LOS	1	5.8	63.5	36.2	180	27
	Tx2 *		Q-LOS	1	8.1	64.6	51.8	196.7	37.1
	Tx3		Q-LOS	1	12	65	41.4	191.2	35.9
	Tx4		NLOS	1	16.7	69.2	44.4	212.9	38.8
	Tx6		NLOS	1	21.3	67.8	49.2	210.9	34.1
	Tx7 *		NLOS	1	16.1	65.2	52.1	202.6	34.2
	Tx5		NLOS	1	18	68.7	49.9	212.2	40
	Tx1 *	Rx2	NLOS	1	12	66.7	47.2	202.8	38.6
	Tx2 *		NLOS	1	7.8	58.5	26	115	15.6
	Tx3		LOS	1	4.9	56.6	30.2	124	17.6
	Tx4 *		LOS	1	6.2	53.5	24.8	107.7	12.9
	Tx7		LOS	1	5.9	52.7	24	72.2	10.8
	Tx5		LOS	1	7.4	55.8	27.7	94.5	14.7
	Tx1	Rx4	NLOS	1	26.1	71.6	45.8	215.1	40.2
	Tx2 *		NLOS	1	21.3	70.3	42.7	215.3	39.3
	Tx3		NLOS	1	16.8	66.4	45.1	201.8	30.9
	Tx4		Q-LOS	1	12.4	63.7	27.3	201.7	23.9
	Tx7		Q-LOS	1	7.8	58.4	30.2	117.6	18.5
	Tx5		Q-LOS	1	10.7	61.3	29.8	116.6	17.7

equal to 1.71 which is overall in good agreement with the results of the studies reported above, for similar frequency bands.

The path loss exponent value obtained in this work is also similar to what found in other investigations at UWB frequencies in residential environment [15], [16]: probably, the heavily cluttered industrial environment we considered shows a similar degree of obstruction despite the larger size of the room. In addition, the results are similar to those ones obtained in [27], where the authors study UWB propagation in a large open indoor environment, i.e. a sports hall.

The value of path loss standard deviation due to shadowing is approximately 4 dB in our measurements, which is in good agreement with the literature. For example, in [10], [19], the authors report shadowing standard deviation values of 4 to 5 dB in the 5.2 GHz band, and around 4 dB at 3.9 GHz in [27]. The average delay spread values (from 9.8 to 49.2 ns) are also in good agreement with the measurements described in [10] and [12].

IV. CONCLUSION

In this work, we present the results of a measurement campaign and a detailed analysis of air-to-ground radio channel characteristics at UWB frequencies. The measurements were conducted in a real, mid-size industrial environment with Tx on a hovering/flying UAV for most cases. Conducted measurements replicate the realistic case of a supervising UAV which is used at the conscious factory to provide visual control for the operational robots and machines.

The main channel characteristics (path gain, delay spread, path-loss exponent, shadowing standard deviation) are analyzed in detail in different propagation conditions (LOS, quasi-LOS and NLOS) and at different heights, both with the UAV hovering in a fixed position and with the UAV flying continuously along the main corridor of the factory. The results presented in this work may be used for link budget calculations and interference analysis. A comparison of "UAV-to-ground" measurements vs. "ground-to-ground" measurements for the same positions shows differences in

the obtained values for some of the considered measurement locations, due to UAV drifting and to the obstruction/scattering effect of the UAV body on the signal.

A literature overview of previous work on UWB channel measurements in factories, large-indoor, and air-to-ground environment is presented in the paper together with a discussion of results. The values found for Path loss exponent, shadowing standard deviation, and RMS Delay Spread, are in agreement to those found in previous work for similar environments and frequencies.

Future work will deal with studies at different frequency bands, including mm-wave bands and with the characterisation of the directional properties of the channel in industrial environment.

ACKNOWLEDGMENT

The authors are grateful to GF automazioni for the opportunity to perform measurements in an operational factory, to Marco Chiani and Davide Dardari of the University of Bologna for providing the UWB boards, and to their students Roberto Cirillo and Vincenzo Nardiello for assisting in the measurement campaign and data post-processing. Part of this work has been completed during the research visit of Vasilii Semkin to University of Bologna.

REFERENCES

[1] Y. Zeng, R. Zhang, and T. J. Lim, "Wireless communications with unmanned aerial vehicles: Opportunities and challenges," *IEEE Commun. Mag.*, vol. 54, no. 5, pp. 36–42, May 2016.

[2] S. A. R. Naqvi, S. A. Hassan, H. Pervaiz, and Q. Ni, "Drone-aided communication as a key enabler for 5G and resilient public safety networks," *IEEE Commun. Mag.*, vol. 56, no. 1, pp. 36–42, Jan. 2018.

[3] S. Hayat, E. Yanmaz, and R. Muzaffar, "Survey on unmanned aerial vehicle networks for civil applications: A communications viewpoint," *IEEE Commun. Surveys Tuts.*, vol. 18, no. 4, pp. 2624–2661, 4th Quart., 2016.

[4] C. Kyrkou, S. Timotheou, P. Kolios, T. Theocharides, and C. Panayiotou, "Drones: Augmenting our quality of life," *IEEE Potentials*, vol. 38, no. 1, pp. 30–36, Jan. 2019.

[5] J. Reimann and G. Sziebig, "The intelligent factory space—A concept for observing, learning and communicating in the digitalized factory," *IEEE Access*, vol. 7, pp. 70891–70900, 2019.

[6] B. Shu, G. Sziebig, and S. Pieskä, "Human-robot collaboration: Task sharing through virtual reality," in *Proc. 44th Annu. Conf. IEEE Ind. Electron. Soc. (IECON)*, Oct. 2018, pp. 6040–6044.

[7] IEEE Standard for Low-Rate Wireless Networks, Standard IEEE Std 802.15.4-2015 (Revision of IEEE Std 802.15.4-2011), 2016, pp. 1–709.

[8] X. Li, J. Timmermann, W. Wiesbeck, and L. Zwirello, *UWB Applications* (EuMA High Frequency Technologies Series). Cambridge, U.K.: Cambridge Univ. Press, 2013, pp. 116–170.

[9] X. Shen, M. Guizani, R. Qiu, and T. Le-Ngoc, *Ultra-Wideband Wireless Communications and Networks*. Hoboken, NJ, USA: Wiley, Feb. 2006.

[10] M.-G. Di Benedetto, T. Kaiser, A. Molish, I. Opperman, C. Politano, and D. Porcino, *UWB Communication Systems. A Comprehensive Overview* (EURASIP Book Series on Signal Processing and Communications). London, U.K.: Hindawi, 2006.

[11] K. Guo, Z. Qiu, C. Miao, A. H. Zaini, C.-L. Chen, W. Meng, and L. Xie, "Ultra-wideband-based localization for quadcopter navigation," *Unmanned Syst.*, vol. 04, no. 01, pp. 23–34, Jan. 2016.

[12] J. Karedal, S. Wyne, P. Almers, F. Tufvesson, and A. F. Molisch, "UWB channel measurements in an industrial environment," in *Proc. IEEE Global Telecommun. Conf. (GLOBECOM)*, vol. 6, Nov. 2004, pp. 3511–3516.

[13] K. Haneda, J.-I. Takada, and T. Kobayashi, "A parametric UWB propagation channel estimation and its performance validation in an anechoic chamber," *IEEE Trans. Microw. Theory Techn.*, vol. 54, no. 4, pp. 1802–1811, Jun. 2006.

[14] L. Greenstein, S. Ghassemzadeh, S.-C. Hong, and V. Tarokh, "Comparison study of UWB indoor channel models," *IEEE Trans. Wireless Commun.*, vol. 6, no. 1, pp. 128–135, Jan. 2007.

[15] L. Rusch, C. Prettie, D. Cheung, Q. Li, and M. Ho, "Characterization of UWB propagation from 2 to 8 GHz in a residential environment," *IEEE J. Sel. Areas Commun.*, Jan. 2003.

[16] S. S. Ghassemzadeh, R. Jana, C. W. Rice, W. Turin, and V. Tarokh, "A statistical path loss model for in-home UWB channels," in *Proc. IEEE Conf. Ultra Wideband Syst. Technol.*, May 2002, pp. 59–64.

[17] M. Radovnikovich, P. Fleck, and K. Hallenbeck, "Ultra wide-band trajectory following for an omnidirectional factory automation vehicle," in *Proc. IEEE Int. Conf. Technol. Practical Robot Appl. (TePRA)*, Apr. 2014, pp. 1–6.

[18] Z. Irahhauten, G. J. M. Janssen, H. Nikookar, A. Yarovoy, and L. P. Ligthart, "UWB channel measurements and results for office and industrial environments," in *Proc. IEEE Int. Conf. Ultra-Wideband*, Sep. 2006, pp. 225–230.

[19] E. Tanghe, W. Joseph, L. Verloock, L. Martens, H. Capoen, K. Herwegen, and W. Vantomme, "The industrial indoor channel: Large-scale and temporal fading at 900, 2400, and 5200 MHz," *IEEE Trans. Wireless Commun.*, vol. 7, no. 7, pp. 2740–2751, Jul. 2008.

[20] A. Kachroo, S. Vishwakarma, J. N. Dixon, H. Abuella, A. Popuri, Q. H. Abbasi, C. F. Bunting, J. D. Jacob, and S. Ekin, "Unmanned aerial Vehicle-to-Wearables (UAV2W) indoor radio propagation channel measurements and modeling," *IEEE Access*, vol. 7, pp. 73741–73750, 2019.

[21] C. Li, E. Tanghe, D. Plets, P. Suanet, J. Hoebeke, E. De Poorter, and W. Joseph, "ReLoc: Hybrid RSSI- and phase-based relative UHF-RFID tag localization with COTS devices," *IEEE Trans. Instrum. Meas.*, vol. 69, no. 10, pp. 8613–8627, Oct. 2020.

[22] H. Deng, Q. Fu, Q. Quan, K. Yang, and K.-Y. Cai, "Indoor multi-camera-based testbed for 3-D tracking and control of UAVs," *IEEE Trans. Instrum. Meas.*, vol. 69, no. 6, pp. 3139–3156, Jun. 2020.

[23] W. Khawaja, I. Guvenc, D. W. Matolak, U.-C. Fiebig, and N. Schneckenburger, "A survey of air-to-ground propagation channel modeling for unmanned aerial vehicles," *IEEE Commun. Surveys Tuts.*, vol. 21, no. 3, pp. 2361–2391, 3rd Quart., 2019.

[24] T. Rappaport, *Wireless Communications: Principles and Practice* (Prentice-Hall Communications Engineering and Emerging Technologies Series), 2nd ed. Upper Saddle River, NJ, USA: Prentice-Hall, 2002.

[25] J. A. Shokouh and R. C. Qiu, "Ultra-wideband (UWB) communications channel measurements—A tutorial review," *Int. J. Ultra Wideband Commun. Syst.*, vol. 1, no. 1, p. 11, 2009.

[26] T. S. Rappaport and C. D. McGillem, "UHF fading in factories," *IEEE J. Sel. Areas Commun.*, vol. 7, no. 1, pp. 40–48, Jan. 1989.

[27] C. Briso, C. Calvo, and Y. Xu, "UWB propagation measurements and modelling in large indoor environments," *IEEE Access*, vol. 7, pp. 41913–41920, 2019.

VASILII SEMKIN received the Lic.Sc. (Tech.) and D.Sc. (Tech.) degrees from the School of Electrical Engineering, Aalto University, in 2014 and 2016, respectively. From 2016 to 2017, he was a Postdoctoral Researcher working on 5G antenna development at Aalto University, and then, at Tampere University of Technology, from 2017 to 2018, studying radio channel properties at mmWave frequencies. From 2018 to 2019, he was a Postdoctoral Researcher with the ICTEAM, Université catholique de Louvain (UCLouvain), Louvain-la-Neuve, Belgium, where he was working on wireless channel characterization, air-to-ground channel measurements, and drone detection. He is currently a Research Scientist with VTT Technical Research Centre of Finland Ltd. His research interests include mmWave channel measurements and modeling, drone-aided communications, radar technology, and reconfigurable antennas.

ENRICO MARIA VITUCCI (Senior Member, IEEE) received the M.Sc. degree in telecommunication engineering and the Ph.D. degree in electrical engineering from the University of Bologna, Italy. From 2011 to 2016, he was a Research Associate with the Center for Industrial Research on ICT, University of Bologna. In 2015, he was a Visiting Researcher at Polaris Wireless Inc., Mountain View, USA. He is currently a Tenure-Track Assistant Professor in electromagnetic fields with the Department of Electrical, Electronic and Information Engineering "G. Marconi" (DEI), University of Bologna. He has authored or coauthored more than 80 technical articles on international journals or conferences, and he is co-inventor of five international patents. His research interests include deterministic wireless propagation models and multi-dimensional radio channel characterization. He is a member of the Editorial Board of the journal *Wireless Communications and Mobile Computing*.

FRANCO FUSCHINI received the M.Sc. degree in telecommunication engineering and the Ph.D. degree in electronics and computer science from the University of Bologna, in March 1999 and July 2003, respectively. He is currently an Associate Professor with the Department of Electrical, Electronic and Information Engineering "G. Marconi," University of Bologna. He has authored or coauthored more than 30 journal articles on radio propagation and wireless system design. His main research interests include the area of radio systems design and radio propagation channel theoretical modeling and experimental investigation. In April 1999, he was a recipient of the Marconi Foundation Young Scientist Prize in the Context of the XXV Marconi International Fellowship Award.

MARINA BARBIROLI received the Laurea degree in electronic engineering and the Ph.D. degree in computer science and electronic engineering from the University of Bologna, in 1995 and 2000, respectively. Since 2020, she has been an Associate Professor with University of Bologna. Her research interests include on propagation models for mobile communications systems, with focus on wideband channel modeling for 5G systems. The research activities includes investigation of planning strategies for mobile systems, broadcast systems and broadband wireless access systems, and analysis of exposure levels generates by all wireless systems and for increasing spectrum efficiency. The research activity includes the participation to European research and cooperation programs, such as COST 259, COST 273 COST2100, COST IC004, and COST IRACON, and the European Networks of Excellence FP6-NEWCOM and FP7-NEWCOM++.

VITTORIO DEGLI-ESPOSTI (Senior Member, IEEE) was a Postdoctoral Researcher with Polytechnic University, Brooklyn, New York (NYU Polytechnic) in the group led by Professor H. L. Bertoni, in 1998. He was a Visiting Professor at Helsinki University of Technology (Aalto University), in 2006, and Tongji University, Shanghai, in 2013. From January 2015 to December 2016, he was the Director of Research of Polaris Wireless Inc., Mountain View, USA. He is currently an Associate Professor with the Department of Electrical Engineering (DEI) of the Alma Mater Studiorum—University of Bologna. He has authored or coauthored about 140 peer-reviewed technical articles in the fields of applied electromagnetics, radio propagation, and wireless systems. He is an Elected Chair of the Propagation Working Group of the European Association on Antennas and Propagation (EuRAAP). He has been the Vice-Chair of the European Conference on Antennas and Propagation (EuCAP), editions in 2010 and 2011, Short-Courses and Workshops Chair of the 2015 Edition, and an Invited Speaker at EuCAP 2014 and International Symposium on Antennas and Propagation (ISAP) 2020, and the Short-Courses Chair of the European Conference on Networks and Communications, (EuCNC) 2020. He is an Associate Editor of the journals *Radio Science* and IEEE Access.

CLAUDE OESTGES (Fellow, IEEE) received the M.Sc. and Ph.D. degrees in electrical engineering from the Université catholique de Louvain (UCLouvain), Louvain-la-Neuve, Belgium, in 1996 and 2000, respectively. In January 2001, he joined as a Postdoctoral Scholar with the Smart Antennas Research Group (Information Systems Laboratory), Stanford University, CA, USA. From January 2002 to September 2005, he was associated with the Microwave Laboratory UCLouvain, as a Postdoctoral Fellow of the Belgian Fonds de la Recherche Scientifique (FRS-FNRS). From 2016 to 2020, he chaired COST Action IRACON. He is currently a Full Professor with the Department of Electrical Engineering, Institute for Information and Communication Technologies, Electronics and Applied Mathematics (ICTEAM), UCLouvain. He has authored or coauthored three books and more than 200 journal articles and conference communications. He was a recipient of the 1999–2000 IET Marconi Premium Award and the IEEE Vehicular Technology Society Neal Shepherd Award, in 2004 and 2012.